

## Constraints on Cold Dark Matter in the Gamma-ray Halo of NGC 253

R. Enomoto<sup>1</sup>, T. Yoshida<sup>2</sup>, S. Yanagita<sup>2</sup>, and C. Itoh<sup>3</sup>

enomoto@icrr.u-tokyo.ac.jp

### ABSTRACT

A gamma-ray halo in a nearby starburst galaxy NGC 253 was found by the CANGAROO-II Imaging Atmospheric Cherenkov Telescope (IACT). By fitting the energy spectrum with expected curves from Cold Dark Matter (CDM) annihilations, we constrain the CDM-annihilation rate in the halo of NGC 253. Upper limits for the CDM density were obtained in the wide mass range between 0.5 and 50 TeV. Although these limits are higher than the expected values, it is complementary important to the other experimental techniques, especially considering the energy coverage. We also investigate the next astronomical targets to improve these limits.

*Subject headings:* galaxy: individual (NGC 253)— gamma rays: theory — dark matter

### 1. Introduction

Recently, the gamma-ray halo in the nearby starburst galaxy NGC 253 was detected by CANGAROO-II (Itoh et al. 2002, 2003a). Although it seems to be successful to interpret it as a high-energy cosmic-ray halo (Itoh et al. 2003b), we assumed that this radiation is due to cold dark matter (CDM) annihilation, and obtained the upper limits of the CDM density in a wide mass range around TeV,

---

<sup>1</sup>Institute for Cosmic Ray Research, University of Tokyo, Chiba 277-8582, Japan

<sup>2</sup>Faculty of Science, Ibaraki University, Ibaraki 310-8512, Japan

<sup>3</sup>Ibaraki Prefectural University of Health Sciences, Ibaraki 300-0394, Japan

The motivation of this study is the morphology obtained in a TeV gamma-ray observation (Itoh et al. 2002, 2003a). It marginally differed from a disk shape. Considering the existence of this halo (Ostriker & Peebles 1973), it would be worth obtaining the constraint of CDM by using the observed TeV emissions.

In this paper we assumed two processes: inclusive gamma-ray production via the annihilation of weakly interacting massive particles to quark anti-quark pairs (Rudaz & Stecker 1988), and monochromatic gamma-rays from the annihilation to two gamma state (Bergström & Snellman 1988). The former final states produce highly multiple gamma-rays and gave better upper limits than the latter method. The final-state gamma-rays would show an exponential energy spectrum which differs from the usually known cosmic-ray spectrum, i.e., a power law.

## 2. Property of NGC 253

The nearby starburst galaxy NGC 253 is located inside the Sculptor group, and can be clearly seen from the southern hemisphere. The distance was estimated to be 2.5 Mpc (de Vaucouleurs 1978). It was classified as SABc (Hubble classification), and is one of the closest examples of “our Galaxy-like object”. It is “edge-on”, i.e., suitable to distinguish its halo from the disk. The optical (Beck et al. 1982) and radio halos (Hummel et al 1984; Carilli et al. 1992) were previously observed in this galaxy, the sizes of which ( $\sim 10$  kpc) approximately agreed with a TeV-gamma-ray observation (13 - 26 kpc) (Itoh et al. 2003a).

HI studies on the Sculptor group galaxies were carried out (Puche & Carignan 1991). Calculating the rotation curves, they concluded that many galaxies in this group have massive halos. Especially, that of NGC 253 was estimated to have a density of  $0.015 M_{\odot} \text{pc}^{-3}$  with a radius of 26.9 kpc, which is also within the size estimation of the TeV-gamma-ray halo (Itoh et al. 2003a).

## 3. Energy spectrum and mass of CDM

The spectral energy distribution (SED) of GeV-TeV gamma rays is plotted in Fig. 1. The points with error bars were obtained by CANGAROO-II (Table 6 of Itoh et al. (2003a)). The arrows are upper limits obtained by EGRET (Streekmar et al. 1994; Blom et al. 1999). According to a theoretical estimation motivated by the cosmic-ray radiation (Itoh et al. 2003b), neither a simple power-law spectrum ( $\propto E^{-\gamma}$ ) of cosmic-rays (curve-A) nor that with a high energy cutoff ( $\propto E^{-2} e^{E/E_{max}}$ ) (curve-B: due to  $\pi^0 \rightarrow \gamma\gamma$  decays or

bremsstrahlung) could simultaneously explain both data. These curves can be well fitted to the TeV data, however, they are inconsistent with the GeV upper limits. The only choice to satisfy both data was inverse Compton scattering oriented by very hard incident electrons ( $\propto E^{-1.5}e^{\sqrt{E}/b}$ ) (curve-C), which may require another mechanism of re-acceleration in the galactic halo.

Fig. 2 shows a semi-log plot of the differential flux of TeV gamma-rays. The line-E is the best-fitted exponential function ( $\propto e^{-aE}$ ), and shows an agreement. The extrapolation to GeV region is well below the EGRET upper limits.

The exponential function has a physical scale (in this case energy scale) and its contribution in the GeV region is negligibly small in SED. The well-known physical process to obtain an energy scale is a fragmentation function ( $\frac{1}{\sigma_h} \cdot \frac{d\sigma}{dx}$ , where  $x$  is a Feynman  $x$ ) for such an inclusive particle spectrum as  $e^+e^- \rightarrow q\bar{q} \rightarrow \gamma X$ . It is typically to be fitted with the sum of the exponential functions. The fragmentation function of LEP data ( $e^+e^-$  collider experiment at the center of mass energy of  $\sim 90$  GeV) (Ackerstaff et al. 1998) was well-fitted with the sum of three exponential functions:

$$\begin{aligned} \frac{1}{\sigma_h} \cdot \frac{d\sigma}{dx} &= e^{5.5605-34.482x} + e^{3.1777-10.551x} \\ &+ e^{7.2391-123.29x}. \end{aligned}$$

Introducing the energy scale  $M_\chi$ , the relationship between  $x$  and the energy of gamma-ray becomes  $x = E/M_\chi$ . The annihilation rate ( $F$  [ $\text{cm}^{-2}\text{s}^{-1}$ ]) and the energy scale were obtained by fitting the TeV-gamma-ray's spectrum with  $\frac{F}{\sigma_h} \cdot \frac{d\sigma}{M_\chi \cdot dx}$  to be

$$\begin{aligned} F &= (1.8 \pm 1.1) \times 10^{-11} [\text{cm}^{-2}\text{s}^{-1}], \\ M_\chi &= (3.0 \pm 0.6) [\text{TeV}], \end{aligned}$$

where we used the TeV gamma-ray fluxes from Table 6 in Ref. (Itoh et al. 2003a). Note that these two parameters are highly anti-correlated, which will be reflected in further analysis, i.e., described later. Here,  $F$  is the observed annihilation rate per unit area and time at Earth. The result is shown by line-D in Fig. 1. The  $\chi^2$  obtained in this fitting was 1.0/D.O.F=4. The EGRET upper limits are also cleared.

For the reaction of CDM to  $\gamma\gamma$  (i.e.,  $\chi\chi \rightarrow \gamma\gamma$ ), the monochromatic gamma-rays were suggested to be searched (Bergström & Snellman 1988; Bouquet et al. 1989; Jungman & Kamionkowski 1995). The energy resolution of TeV gamma-rays is approximately 35% (Table 5 of Itoh et al. (2003a)). The curve-F in Fig. 2 is an example of a Gaussian ( $\propto e^{-\frac{1}{2}\left(\frac{E-M_\chi}{\sigma_E}\right)^2}$ ) with that resolution and a center value of 0.7 TeV.

#### 4. Upper limit for the number density of CDM

The annihilation in the volume of the halo should be detected at a rate of

$$F = \langle \sigma v \rangle B_{q\bar{q}} n^2 [V / (4\pi d^2)],$$

where  $\sigma$  is the annihilation cross section,  $v$  the relative velocity of CDMs,  $B_{q\bar{q}}$  the branching fraction of  $\chi\chi \rightarrow q\bar{q}$ ,  $n$  the number density of CDM,  $V$  the total volume of the halo, and  $d$  the distance from Earth.

Here, we consider the last volume-distance factor. The dark halo size of NGC 253 obtained by an HI measurement is 26.9 kpc (Puche & Carignan 1991), which corresponds to a solid angle of  $\Delta\theta = 0.62^\circ$ . Thus the volume factor becomes  $\frac{d}{3} \cdot (\Delta\theta)^3$ , proportional to the distance. When we see the same-angular-sized diffuse image, it suggests that distant objects have advantages. For example, comparing the Galactic Center (distance of 8.5 kpc) and NGC 253, this factor becomes 300. Although the Galactic Center may have a CDM concentration factor of, say, 1000 (Navarro et al. 1996), it is highly model dependent. On the other hand, the total volume average of the squared density is less model dependent (only a factor changes under the assumption of  $r^{-n}$ ,  $n=0,1,\dots$ ).

The annihilation cross section is another source of model dependences. For example, whether CDM is Dirac or Majorana fermion. Also, it depends on the details of particle physics, i.e., the details of SUSY breaking (Jungman et al. 1996). A much larger dependence is expected to the  $\chi\chi \rightarrow \gamma\gamma$  process. In order to avoid it, we carried out the following. According to the Lee-Weinberg equation of the CDM density evolution (Lee & Weinberg 1977; Jungman et al. 1996), the annihilation cross section is directly related to the cosmological abundance of  $\Omega_{CDM}$ ,

$$\Omega_{CDM} = 7 \times 10^{-27} [\text{cm}^3 \text{s}^{-1}] / \langle \sigma v \rangle,$$

which is mass independent. Recently, WMAP determined  $\Omega_{CDM} = 0.23$  (Bennett et al. 2003). With this, we normalized  $\langle \sigma v B_{q\bar{q}} \rangle$  to an order of  $10^{-26} [\text{cm}^3 \text{s}^{-1}]$ .

Now that all of unknown factors have been filled, by fitting the TeV gamma-rays spectrum with the described function, we can derive the best-fitted density for CDM,

$$n = (2.4 \pm 0.6) \times 10^{-2} \sqrt{\frac{10^{-26} \text{cm}^3 \text{s}^{-1}}{\langle \sigma v B_{q\bar{q}} \rangle}} [\text{cm}^{-3}],$$

where  $n$  is still highly correlated with the  $M_\chi$  value. Changing  $n$  to the energy density of the CDM,

$$\rho_{CDM} = (70.8 \pm 7.4) \sqrt{\frac{10^{-26} \text{cm}^3 \text{s}^{-1}}{\langle \sigma v B_{q\bar{q}} \rangle}} [\text{GeV cm}^{-3}]$$

is obtained, where the correlation between  $M_\chi$  and  $\rho_{CDM}$  is shown in Fig. 3. Note that  $n$  and  $\rho_{CDM}$  are the root-mean-squared volume average of those densities. The lines are 1- and 2- $\sigma$  contours. The reasons why the errors became smaller compared to the value of  $F$  are because  $\rho_{CDM}$  is proportional to  $\sqrt{F}$  and there is a strong anti-correlation between  $F$  and  $M_\chi$ .

To summarize, the final fitting data and functions are as follows:

$$\begin{aligned} \left[ \frac{dF}{dE} \right] &= \frac{F}{M_\chi} \cdot \left[ \frac{1}{\sigma_h} \cdot \frac{d\sigma}{d(E/M_\chi)} \right] \\ &= \frac{\langle \sigma v B_{q\bar{q}} \rangle n^2 [V/(4\pi d^2)]}{M_\chi} \\ &\quad \cdot \left[ \frac{1}{\sigma_h} \cdot \frac{d\sigma}{d(E/M_\chi)} \right] \\ &= \frac{\langle \sigma v B_{q\bar{q}} \rangle \rho_{CDM}^2 [V/(4\pi d^2)]}{M_\chi^3} \\ &\quad \cdot \left[ \frac{1}{\sigma_h} \cdot \frac{d\sigma}{d(E/M_\chi)} \right], \end{aligned}$$

where  $[\frac{1}{\sigma_h} \cdot \frac{d\sigma}{d(E/M_\chi)}]$  should be replaced with the linear combination of three exponential functions described so far and  $[\frac{dF}{dE}]$  are Table 6 of Itoh et al. (2003a) and Fig. 1 of Blom et al. (1999), respectively.

Although, these values are the best-fitted ones, there are not enough reasons to insist that this is evidence for CDM other than that the energy spectrum was fitted well with the exponential function. This value should be considered to be an upper limit. We, therefore, carried out a scan for various  $M_\chi$  assumptions, and obtained upper limits versus  $M_\chi$ . The results are shown in Fig. 4. Considering the dynamic range of the fragmentation function measurements, the searched range was selected to be from 0.5 to 50 TeV. In the figure, the 2 $\sigma$ -upper limits are shown. The improvement below 0.65 GeV was due to the EGRET upper limits.

In addition, we carried out a search for monochromatic gamma-rays in the energy region between 0.5 and 3 TeV. The TeV gamma-ray energy spectrum was fitted with Gaussians under various peak-energy assumptions. A uniform energy resolution of 35% was assumed. A typical line is shown in Fig. 2 (line-B). The 2 $\sigma$ -upper limits for the mass densities of CDM,  $\rho_{CDM} \sqrt{\frac{10^{-29} \text{cm}^3 \text{s}^{-1}}{\langle \sigma_{\gamma\gamma} v \rangle}}$ , were obtained ( Fig. 5 ). Here we used a smaller normalization factor for  $\langle \sigma_{\gamma\gamma} v \rangle$  as was expected from the particle theory (Bergström & Snellman 1988). These upper limits are higher than these in Fig. 4.

## 5. Discussion

The halo density estimated by the HI studies is  $0.015 \text{ M}_{\odot} \text{pc}^{-3}$  ( $0.57 \text{ [GeVcm}^{-3}\text{]}$ ) (Puche & Carignan 1991), which is two orders lower than our upper limits. The gamma-ray flux from NGC 253 should be explained by the standard cosmic-ray theory. Due to the starburst phenomena, we could not throw away a cosmic-ray interpretation (Völk et al. 1996). If the cosmic-ray emission is accurately determined from the study of multi-wavelength spectrum, this upper limit will be greatly reduced to the error-bar level.

A scan of the nearby galaxies that are not starburst will be promising in the search for CDM. Especially, the Sculptor group is an interesting target, which is also suggested by an HI measurement (Puche & Carignan 1991).

The search for gamma-rays from massive galaxies is considered to reduce the upper limit for the galactic density of CDM. Ten-times-heavier astronomical objects that are nearby, would give a sensible result. For example, M 87 is considered to be more than ten-times heavier than our Galaxy (Baltz et al. 2000). The distance is several-times farther than NGC 253. The volume-distance factor,  $\frac{d}{3} \cdot (\Delta\theta)^3$ , is, therefore, an order lower than our case (reported  $\Delta\theta < 0.127^{\circ}$  (Aharonian et al. 2003a)). On the other hand, the recent observation by HEGRA reported about a ten-times fainter gamma-ray intensity (Aharonian et al. 2003a). These values should result in the same order of CDM density, while M87's density is considered to be larger than that of NGC 253. Publication of the differential flux of the TeV gamma-ray from M87 is awaited.

Although M 31 is also massive, the visible size is larger than the field of view of IACTs, which requires special treatments for background subtractions (Aharonian et al. 2003b).

Considering a figure of merit (*FOM*) for the CDM search, we had better consider total mass of galaxy, volume of halo, distance, and visible size simultaneously. The CDM density may be proportional to the total mass ( $M_G$ ) divided by the volume. Thus, the expected gamma-ray's flux should be proportional to the following:  $FOM = M_G^2 d^{-5} (\Delta\theta)^{-3}$ . Selecting those nearby galaxies that have a visible size of between  $3 \times 10^{-3}$  and  $10^{-2}$  radian (favorable size for the IACT measurements), NGC 5128 (Cen-A) and NGC 5236 (M 83) were calculated to have a bigger *FOM* than that of NGC 253. Especially for Cen-A, hundred-times larger flux is expected.

We also applied the same discussion to  $\omega$ -Centauri (Guy et al. 2002). The dark matter origin of globular clusters was proposed by Peebles (1984). The distance is close and lower cosmic-ray level is expected. The *FOM* was calculated to be 10000 times higher than that of NGC 253. An upper limit which is the same order with the baryonic density could be obtained.

Also, a high-sensitivity search in the Galactic Center is awaited (Tsuchiya et al. 2003). However, to remove the model dependence and to estimate the cosmic-ray there are keys for this case.

Compared to the accelerator experiment, only IACT measurements are sensitive to CDM with a mass heavier than TeV. They are complementary important to each other.

## 6. Conclusion

A constraint on the cold dark matter (CDM) was obtained using the data of the gamma-ray halo around the nearby starburst galaxy NGC 253. According to this study, upper limits for the CDM density were obtained in the mass range between 0.5 and 50 TeV. Although these limit is higher than the expected value, this is one of first trials from the IACT observational side. The IACTs have been proven to have abilities to detect it. The presently existing IACTs are competitive devices compared with high-energy particle accelerators. The nearby galaxies such as NGC 5128 (Cen-A) and NGC 5236 (M 83) and / or globular cluster  $\omega$ -Centauri will be next interesting targets. Observational efforts for probable candidates should be systematically continued.

We thank Prof. J. Hisano and Prof. M. Fukugita of ICRR for various discussions.

## REFERENCES

- Ackerstaff, K., et al. 1998, *Eur. Phys. J. C*5, 411
- Aharonian, F., et al. 2003a, submitted to *A&A*, astro-ph/0302155
- Aharonian, F.A., et al., 2003b, submitted to *A&A*, astro-ph/0202347
- Baltz, E.A., et al., 2000, *Phys. Rev. D* 61, 023514
- Beck, R., Hutschenreiter, G., & R. Wielebinski, R. 1982, *A&A*, 106, 112-114
- Bennett, C.L., et al. 2003, astro-ph/0302207
- Bergström, L. & Snellman, H., 1988, *Phys. Rev. D*37, 3737
- Blom, J.J., Paglione, T.A.D., & Carraminana, A. 1999, *ApJ*, 516, 744
- Bouquet, A., Salati, P., & Silk, J. 1989, *Phys. Rev. D*40, 3168

- Carilli, C.L., Holdaway, M.A., & Ho, P.T.P. 1992, C.G. de Pree, ApJ, 399, L59
- de Vaucouleurs, G. 1978, ApJ, 224, 710
- Guy, J., for the H.E.S.S. collaboration, 2002, proceedings of 4th Int. WS. on the identification of Dark Matter, Sept. 2002, York, England
- Hummel, E., Smith, P., & van der Hulst, J.M. 1984, A&A, 137, 138
- Itoh, C., Enomoto, R., Yanagita, S., Yoshida, T., et al. 2002, A&A, 296, L1-4
- Itoh, C., Enomoto, R., Yanagita, S., Yoshida, T., et al. 2003a, A&A, 402, 443-455
- Itoh, C., Enomoto, R., Yanagita, S., Yoshida, S., & Tsuru, T.G. 2003b, ApJ, 584, L65-68
- Jungman, G. & Kamionkowski, M. 1995, Phys. Rev. D51, 3121
- Jungman, G., Kamionkowski, M., & Griest, K. 1996, Phys. Rep., 267, 195
- Lee, B.W. & Weinberg, S. 1977, Phys. Rev. Lett., 39, 165-168
- Navarro, J.F., Frenk, C.S., & White, S.D.M. 1996, ApJ. 462, 563
- Ostriker, J.P. & Peebles, P.J.E., 1973, ApJ, 186, 467-480
- Peebles, P.J.E., 1984, ApJ, 277, 470-477
- Puche, D. & Carignan, C. 1991, ApJ, 378, 487-495.
- Rudaz, S. & Stecker, F.W. 1988, ApJ, 325, 16-25
- Streekmar, P., et al. 1994, ApJ, 426, 105
- Tschiya, K., Enomoto, R., et al., 2003, Proc. on "The Universe Viewd in Gamma-rays", Univ. of Tokyo Symposium, Universal Academy Press, Tokyo, Japan, pp229-234
- Völk, H.J., Aharonian, F.A., & Breitschwerdt, D. 1996, Space Sci. Rev. 75, 279



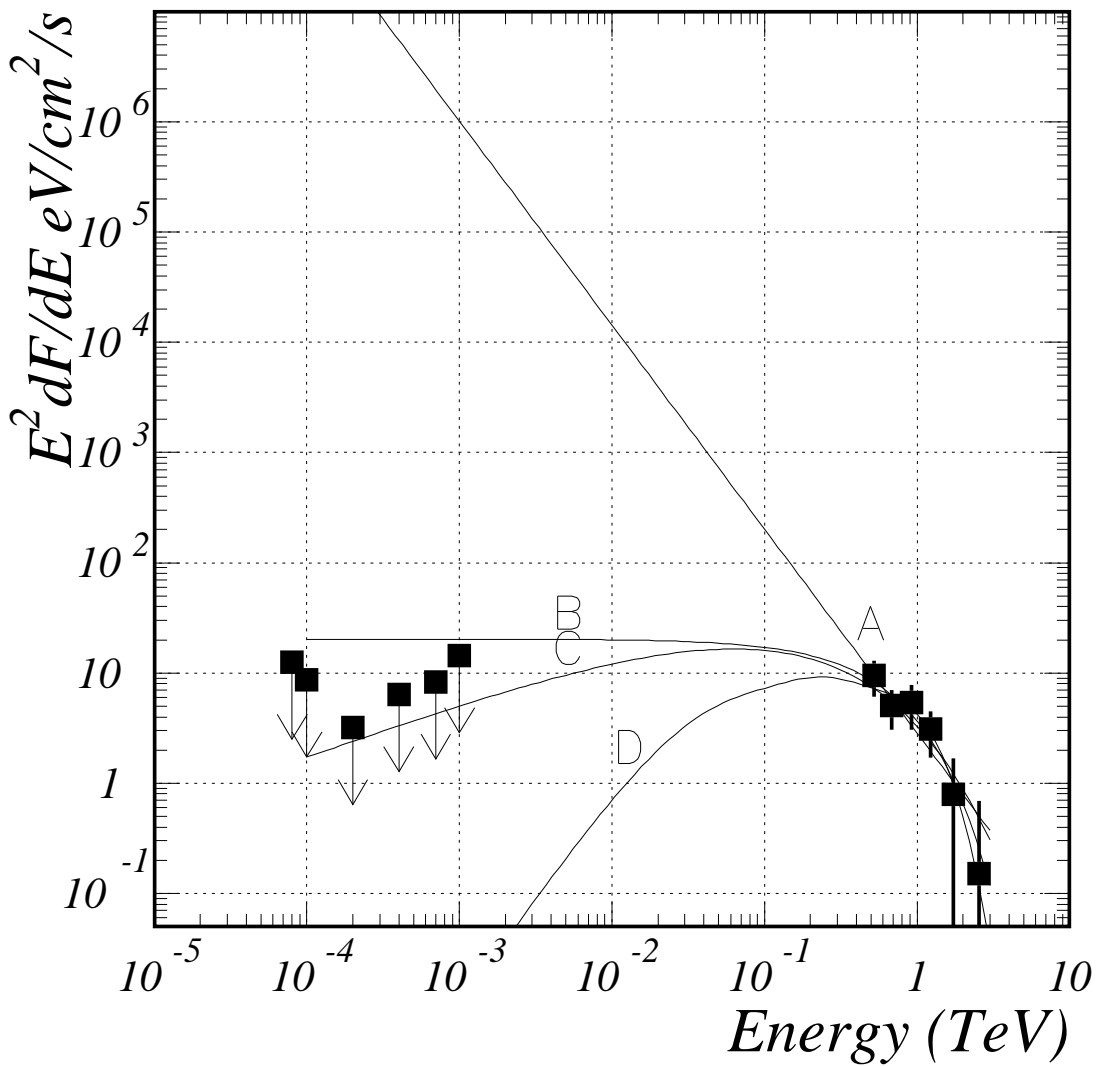


Fig. 1.— Spectral energy distribution. The high-energy data were obtained by CANGAROO-II and the low-energy upper limits by EGRET. The lines are the results of various fitting functions describe in the text.

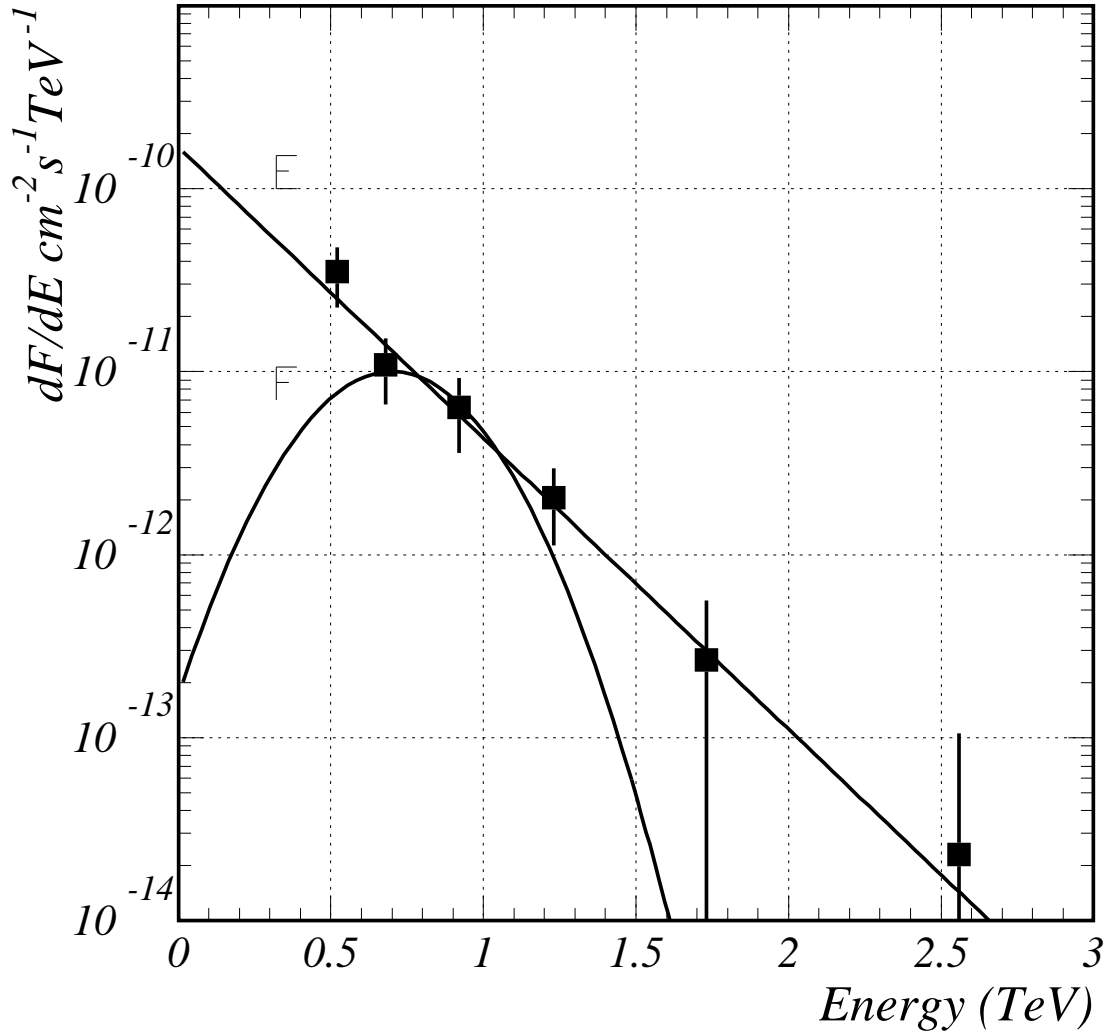


Fig. 2.— Differential flux of gamma-rays from NGC 253 in the semi-log scale. The data were obtained from CANGAROO-II. Line-E is the best-fitted exponential curve and line-F is an example of a Gaussian with an energy resolution of 35% and a center value of 0.7 TeV.

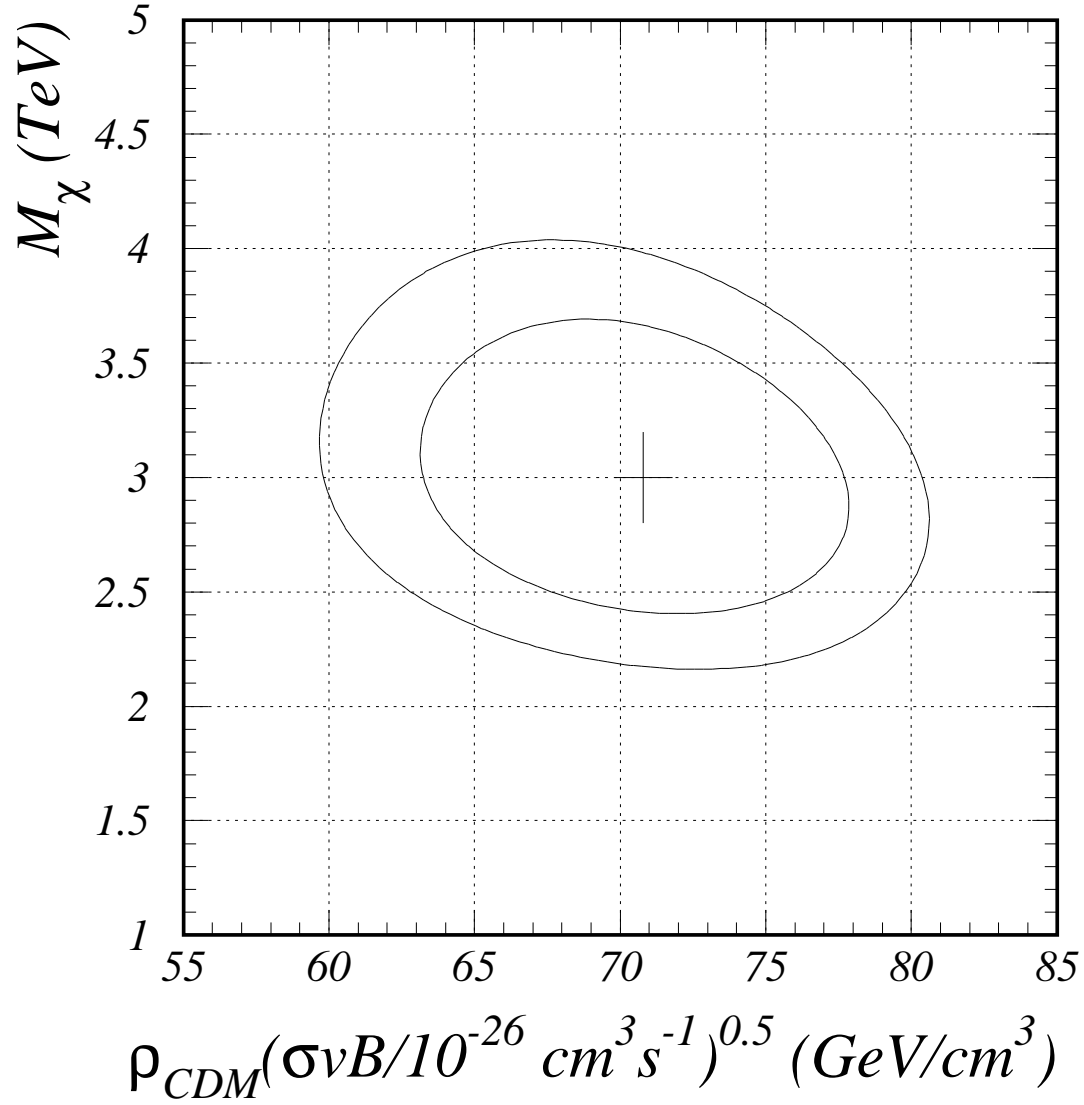


Fig. 3.— Correlation between  $M_\chi$  and  $\rho_{CDM}$ . 1- and 2- $\sigma$  contours are shown with the cross corresponding to the best-fitted value.

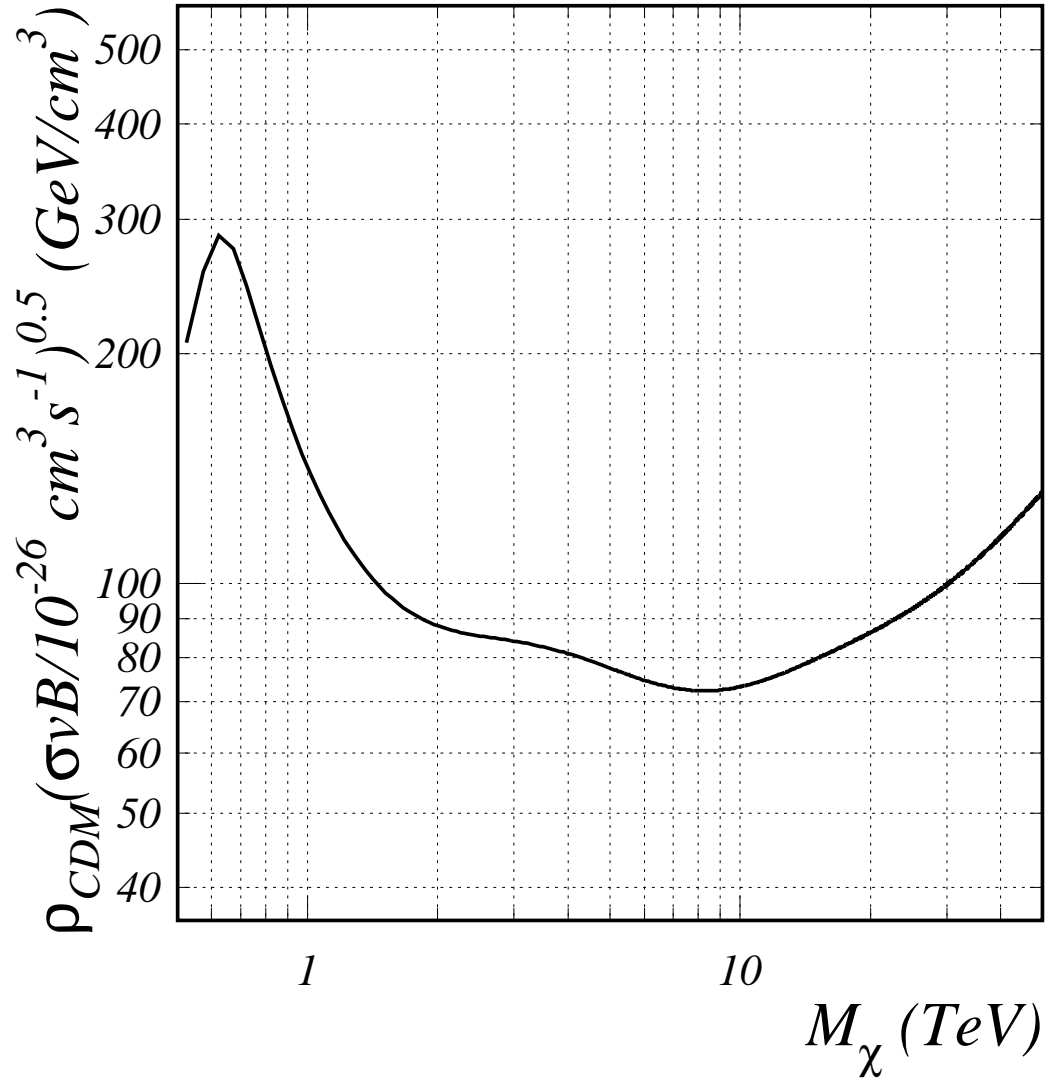


Fig. 4.—  $2\sigma$ -Upper limits of  $\rho_{CDM}$  versus  $M_\chi$  for various  $M_\chi$  assumptions.

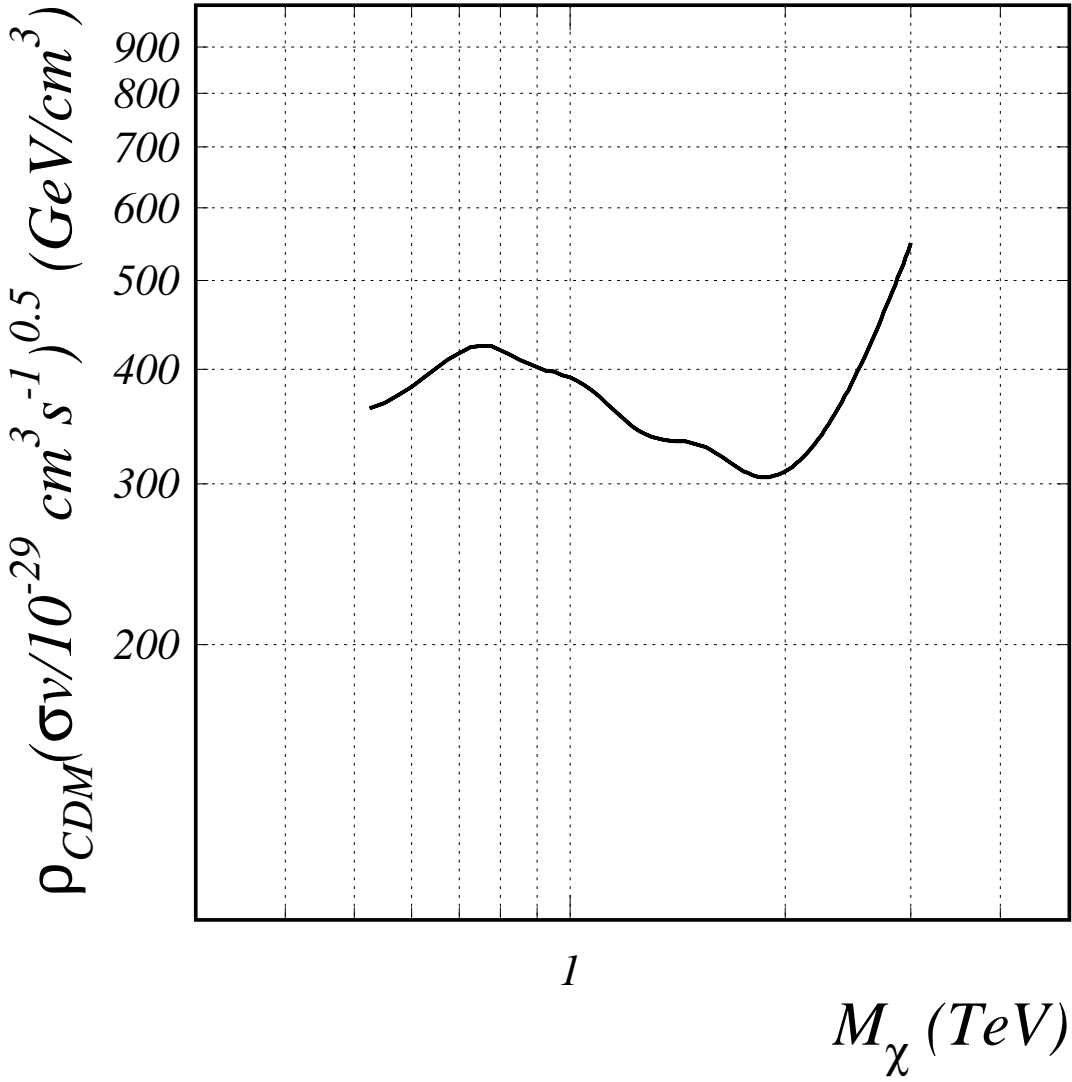


Fig. 5.— Upper limits of  $\rho_{CDM}$  versus  $M_\chi$ . Here, a monochromatic gamma-ray search was carried out for the reaction  $\chi\chi \rightarrow \gamma\gamma$ .